Ultrawide-Band Radar Observations of Multipath Propagation Over the Sea Surface

Mark A. Sletten, *Member, IEEE*, Dennis B. Trizna, *Member, IEEE*, and James P. Hansen, *Member, IEEE*

***Abstract*—An ultrawide-band radar system centered at 10 GHz has been developed for sea-scatter research and was recently deployed on a research pier in the North Atlantic. The radar is based on a time-domain reflectometer module for a sampling oscilloscope. Using transient excitation of a traveling wave-tube amplifier, the system generates 200-ps wide pulses with a 10-GHz center frequency and a peak power of approximately 1 KW. The resulting range resolution is approximately 3 cm. The system was used to investigate low-grazing angle, multipath effects in the ocean environment using a trihedral corner reflector, mounted 45 cm above the water surface. The ultrahigh-range resolution of the system allows spatial separation of the direct and indirect echoes from the trihedral. In addition, a comparison of the indirect vertically- (VV) and horizontally- (HH) polarized echoes illustrates the effects of Brewster angle damping. The implications of these effects for sea-clutter statistics are briefly discussed.**

I. Introduction

MULTIPATH propagation has long been recognized as an important consideration when operating radar systems at sea. At low-grazing (high-incidence) angles, energy which travels to or from the target via forward scatter off the sea surface may combine coherently with energy which follows a direct path, causing signal amplitude and phase variations. This phenomena reduces the ability of systems to track targets at low-grazing angles, and much research has been conducted to mitigate its effects [1]. Recently, the role of multipath propagation in the *generation of sea clutter* has also been the subject of study. Although its role was earlier inferred by Long [2], Lee *et al.* [3] have recently postulated that it may account for the polarization-ratio anomalies they observe in sea-scatter data collected off the coast of Scotland. Trizna [4] recently incorporated a multipath scattering mechanism into a clutter model and showed how it can account for the major differences observed between the amplitude characteristics of horizontally- (HH) and vertically- (VV) polarized backscatter. Sletten [5], [6] has also found strong evidence of a multipath scattering mechanism in the backscatter from breaking waves in a laboratory wavetank.

One way to determine the role of multipath in the generation of sea scatter is to collect ocean backscatter data with a radar capable of resolving the direct and indirect components of the scattered field. With a sufficiently high degree of range resolution, the components of the multipath signal can be observed directly. Many research groups involved in ultrawide-band radar research have developed laboratory systems with subdecimeter resolution (for example, see [7]), but field systems, particularly those deployed at sea, do not have the range resolution necessary to resolve multipath echoes in a two-way, monostatic configuration. In [5] and [6], a short pulse, ultrawide-band radar was used to infer the presence of double-bounce scatter from a breaking water wave, but this was achieved without actually spatially resolving the components of the backscatter.

This paper reports on an experiment in which a modified version of the system used in [5] and [6] was used to demonstrate the spatial resolution of multipath echoes from a target situated close to the sea surface. The objective of the experiment was to demonstrate the ability to resolve multipath echoes at low-grazing angles from a scatterer situated above the surface by a distance commensurate with typical wave heights. In the experiment, backscatter is observed from a trihedral corner reflector, floating approximately 45 cm above the surface of the North Atlantic. The 3-cm range resolution of the radar system used in the experiment allows resolution of the multipath components, even at a grazing angle of 4°. The experiment also demonstrats the effect of Brewster-angle damping on the multipath echoes for VV polarization. Those components of the VV-polarized echo which experienced a reflection at the water surface are seen to be severely attenuated with respect to those scattered directly.

The discussion of the experiment is divided into six sections. Following this introduction, a simple model describing multipath scattering in the time domain is presented. In Section III, the ultrawide-band radar system used to resolve the multipath echoes is briefly described. Experimental results are presented in Section IV, and Section V contains a brief discussion of the relevance of these measurements to sea-scatter research. A short summary can be found in Section VI.

II. A Model for Multipath in the Time Domain

Multipath is a well-known phenomenon which affects radar measurements of targets situated over the earth or the ocean surface. In the marine environment, multipath interference occurs when the echo scattered directly from the target combines coherently with echoes which arrive at and/or return from the target via a path which involves a reflection off the sea surface. For narrowband radar systems, this interference results in enhancement of the backscatter if the two-way path-length difference is approximately a multiple of the radar wavelength, or signal fading if the path difference is near an odd multiple of a half wavelength. These alternate regions of constructive and destructive interference produce lobe patterns as the target height above the surface is varied.

Manuscript received June 19, 1995.

The authors are with the Naval Research Laboratory, Code 7255, Washington, DC 20375 USA.

Publisher Item Identifier S 0018-926X(96)03221-8.

0018–926X/96$05.00 © 1996 IEEE

Authorized licensed use limited to: Perkins Coie LLP. Downloaded on June 24,2025 at 22:07:24 UTC from IEEE Xplore. Restrictions apply.

MEDIATEK-1060
MediaTek Inc. v. ParkerVision, Inc.
IPR2024-00796

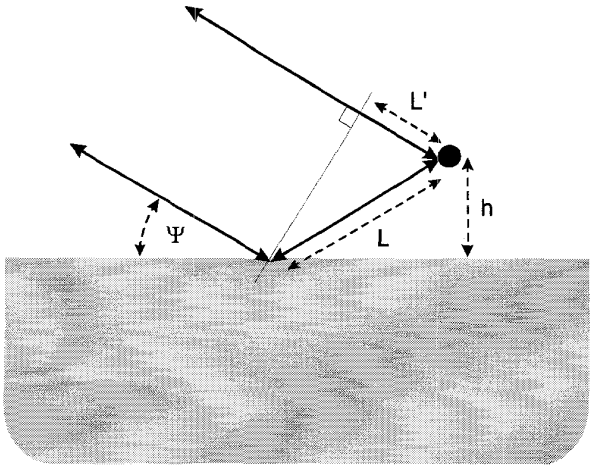


Fig. 1. Schematic diagram illustrating multipath propagation. Four combinations of direct and indirect paths result in three distinct path lengths for two-way propagation; L and L' are the differential path lengths for the indirect and direct paths, respectively.

Calculations of these multipath interference patterns can be found in many radar texts (for example, see [8]). As shown by a conventional narrowband analysis, the backscattered signal $E_{total}(\omega)$ consists of three components

$$E_{tot}(\omega) = E_o S_{dd} e^{i2kL'} + 2E_o R S_{di} e^{ik(L+L')} + E_o R^2 S_{ii} e^{i2kL}. \quad (1)$$

The first term represents energy which follows a direct path to and from the target (direct-direct) and which undergoes a monostatic reflection at the target, indicated by the scattering coefficient S_{dd}. The second term accounts for scattering which experiences a single, specular reflection off the sea surface, indicated by the reflection coefficient R, either in the incident or return path (direct-indirect). Note that this term requires a *bistatic* reflection off the target itself, indicated by the coefficient S_{di}. The final term accounts for scattering which involves a reflection off the ocean surface in both the incident and return path (indirect-indirect), in addition to a monostatic reflection off the target, indicated by S_{ii}. k is the radar wavenumber, and L and L' refer to the differential path lengths for the indirect and direct paths, respectively, as indicated in Fig. 1. From simple geometry

$$L = \frac{h}{\sin\psi}$$
$$L' = L\sin\left[\frac{\pi}{2} - 2\psi\right] \quad (2)$$

where h is the height of the target above the water surface and ψ is the grazing angle. Although not explicitly indicated in (1), the frequency, polarization, and grazing-angle dependence of the reflection and scattering coefficients is assumed.

To the extent that the measurement is linear and time invariant, this analysis can be applied to ultrawide-band measurements on a frequency-by-frequency basis. However, in the case of extremely high range resolution measurements, a time-domain model provides more physical insight into the scattering process. Let the power envelope of the incident waveform be given by $A(t)$. Replacing the phase delays in (1) with corresponding time delays in $A(t)$ produces the following expression for the backscattered echo envelope

$$E_{tot}(t) = A\left(t - \frac{2L'}{c}\right)|S_{dd}| + 2A\left(t - \frac{L+L'}{c}\right)|RS_{di}| + A\left(t - \frac{2L}{c}\right)|R^2 S_{ii}| \quad (3)$$

where c is the velocity of light. It is assumed that while the incident signal is ultrawide-band, the scattering and reflection coefficients do not vary significantly over the RF bandwidth of the radar system. While this may not always be the case, this is a good approximation for the radar system discussed in this paper. Also, pulse distortion due to dispersion in the water and target reflections has been neglected. This approximation is also not generally valid, but it is acceptable under the experimental conditions encountered in this paper (see Section IV). Note that given an incident waveform with sufficient time resolution, time separation of the three components of the scattered field can occur. In particular, if the pulse width W of the incident waveform is smaller than the delay between adjacent components

$$W < \frac{L - L'}{c} = \frac{2h}{c}\sin(\psi) \quad (4)$$

the three contributions to the total echo will be resolved. In this case, interference effects will no longer occur. Rather than observing an enhancement or reduction of the signal, depending on the target height above the surface, the radar will record three distinct echoes with a spacing determined by the target height. Also, changes in the reflection or scattering coefficients due, for example, to polarization or grazing-angle changes, will be observed as variations in the relative strengths of the three echoes rather than simply as changes in the overall cross section of the target.

III. System Description

A block diagram of the radar system used in this investigation is shown in Fig. 2. The core of the radar is a Tektronix 7S12 time-domain reflectometer (TDR) module. The system is similar to a radar developed for laboratory sea-scatter research [5], with the main modification being the insertion of a pulse generator and a traveling wave tube amplifier (TWT) into the transmit channel [9]. (This higher powered system is not presently polarimetric, as is the laboratory system.) The fast rise-time (15-ps) voltage step produced by the PSPL 4015B pulse generator excites the 6– to 18-GHz TWT producing a microwave pulse with a 10-GHz center frequency and a 3-dB bandwidth of approximately 4 GHz. The output pulse produced by the TWT and its associated RF spectrum can be seen in Fig. 3(a) and (b), respectively. The waveform consists of two to three cycles at 10 GHz, resulting in a 3-dB pulse width of approximately 200 ps, and a corresponding range resolution of approximately 3 cm. The peak power level of the pulse is approximately 1 KW, although subsequent losses in the cabling for the antenna system reduce the radiated power by approximately 3 dB.

Authorized licensed use limited to: Perkins Coie LLP. Downloaded on June 24,2025 at 22:07:24 UTC from IEEE Xplore. Restrictions apply.

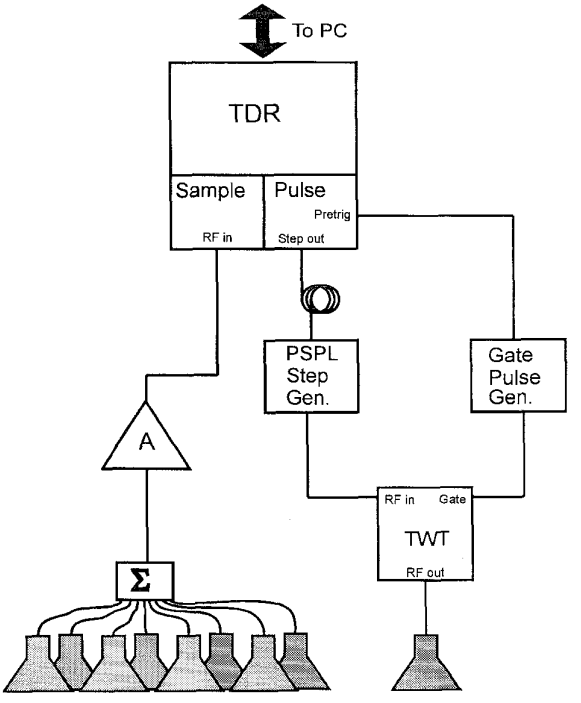


Fig. 2. Block diagram of the ultrawide-band radar used in the multipath measurements.

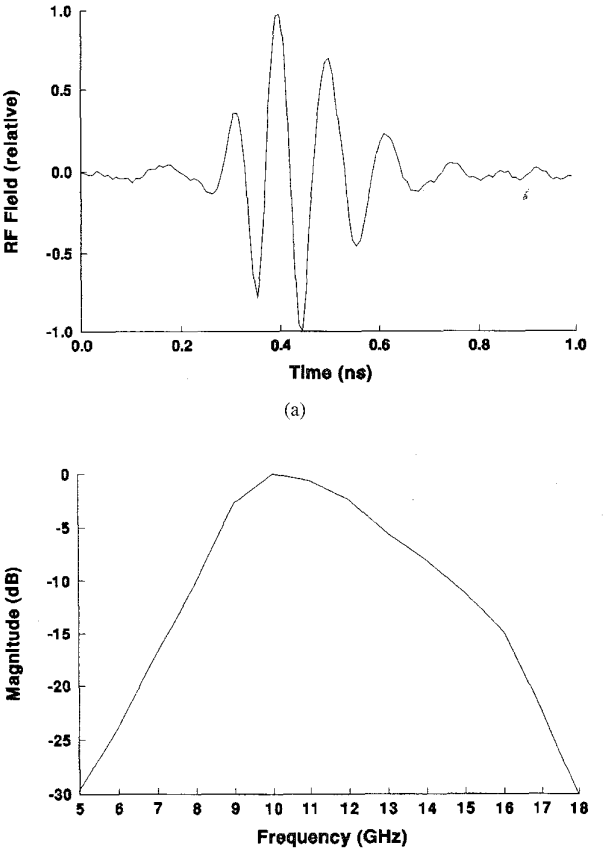


Fig. 3. (a) RF pulse produced by the TWT and (b) its corresponding RF spectrum.

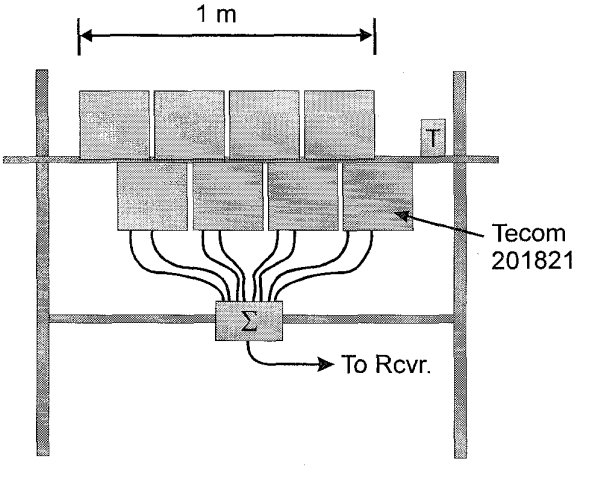


Fig. 4. Diagram of the eight-element ultrawide-band receive array.

Separate antennas are used for transmitting and receiving. To reduce the system beamwidth, an 8-element array has been developed for the receive channel. A sketch of the receive array can be found in Fig. 4. The antenna consists of eight Tecom 201821 horns arranged in a staggered, "quasi-linear" configuration, with a total length of 1 m. The Tecom antenna was chosen on the basis of its wide bandwidth (2–18 GHz), low-pulse distortion, dual polarization, and commercial availability. The outputs of the 8 elements are routed through delay-matched coax lines to an 8-port combiner, producing an array with a beamwidth of less than 2° (at 10 GHz), fixed at 90° relative to the array axis. Field measurements were used to determine the beamwidth and to verify that any sidelobe levels were 15 dB or more down from the main beam (a single Tecom horn has a 3-dB beamwidth of approximately 10° at 10 GHz). The antenna can be set to receive vertical or horizontal polarization through the choice of orthogonal feeds present on each element. A separate antenna, an x-band standard gain horn, is used in the transmit channel. While not designed as an ultrawide-band radiator, the short-pulse response of the standard gain horn is acceptable for the purposes of this research.

After reception by the antenna array, the signal is amplified by a 6- to 12-GHz receive amplifier and then sampled by the sample head of the TDR module. The TDR unit utilizes equivalent time sampling to build up the RF echo produced by the target. In this technique, samples from successive pulses, shifted from one another in range by fractions of a wavelength, are combined to generate a composite, "equivalently time-sampled" pulse. Typically, 128 samples over a 1-ns (equivalent) time period are used to construct the RF pulse, resulting in an effective sampling rate of 128 GHz. Each equivalently-sampled pulse is built up over 2.5 ms of actual time, and an additional recovery interval of 1 ms results in an effective-system pulse repetition interval of 3.5 ms. Data acquisition and system timing are controlled by commercially available plug-in boards in a personal computer.

Authorized licensed use limited to: Perkins Coie LLP. Downloaded on June 24,2025 at 22:07:24 UTC from IEEE Xplore. Restrictions apply.

IV. Trihedral Corner Reflector Measurements

To investigate multipath scattering effects in the ocean environment, a simple experiment involving a floating target was conducted. The radar system was deployed on a research pier at the Coastal Engineering Research Center, near Duck, NC. As sketched in Fig. 5, the target for the experiment consisted of a cluster of triangular trihedral corner reflectors mounted on the top of a floating, tethered staff. The trihedrals measured 30 cm on a side, and the apexes of the trihedrals were located approximately 45 cm above the mean water surface. After anchoring the target in 7 m of sea water, the backscatter from the target for both VV and HH polarizations was measured. The target range and antenna-to-surface height were 110 m and 7.5 m, respectively, producing a grazing angle of 4°. Winds were calm during the measurements, although a light swell was present which tended to gently rock and slowly rotate the trihedral cluster. Using the model outlined in the previous section, the echo separation between adjacent components of the multipath signal should be approximately 0.25 ns. Available measurements and calculations of the cross section of the trihedral at a bistatic angle of 8° indicate that S_{di} should suppress the indirect-direct (second) echo by at least 15 dB, relative to the direct-direct and indirect-indirect echoes [10], [11]. However, the signal-to-noise ratio for this measurement was only approximately 15 dB (using the peak of the first echo as a measure of the signal strength), and thus, the indirect-direct echo should lie near or beneath the system noise. In addition, the polarization dependence of the sea-water reflection coefficient, a result of Brewster-angle damping of the VV-polarized signal, should be evident as well. At 4° grazing, $|R_H| \approx 1$ and $|R_V| \approx 0.37$ [12]. Thus, the third echo for VV polarization should be approximately 17 dB below the first, a level which is again below the system noise. The HH-backscattered signal should therefore appear as a pair of echoes—the direct-direct and the indirect-indirect—separated by 0.5 ns, while the VV signal should consist of a single echo—the direct-direct component. Over the 8- to 12-GHz band, the phase retardation of the water-reflection coefficient at this grazing angle is close to 180°, and thus, the reflection at the water surface should produce only an inversion rather than a distortion. This inversion has little or no impact on the power envelope displays (shown below), and thus, can be neglected for the purposes of this paper. Pulse distortion due to the reflection off the trihedral itself is also negligible, as determined by many other measurements conducted in the absence of multipath.

Fig. 6 contains a typical range-time plot of the experimental data. The received echo envelope, encoded in a linear grey scale, is plotted for VV and HH polarizations. The range extent shown is 15 cm, corresponding to 1 ns of delay. The envelopes of 400 waveforms are plotted for a total time extent of 1.4 seconds. The difference between the echoes for the two polarizations is striking. The HH signal consists of a pair of echoes with a spacing of approximately 0.5 ns, as predicted by the simple analysis outlined in the previous section. The two HH echoes are of approximately the same strength and both undergo some modulation in amplitude. As determined

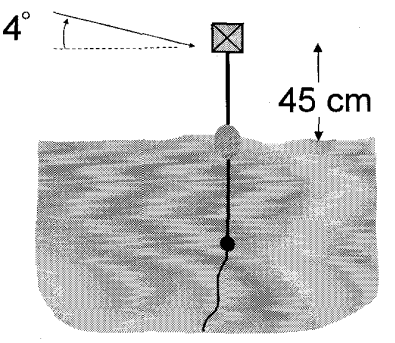


Fig. 5. Diagram of the trihedral corner reflector cluster used as a target in the multipath experiments.

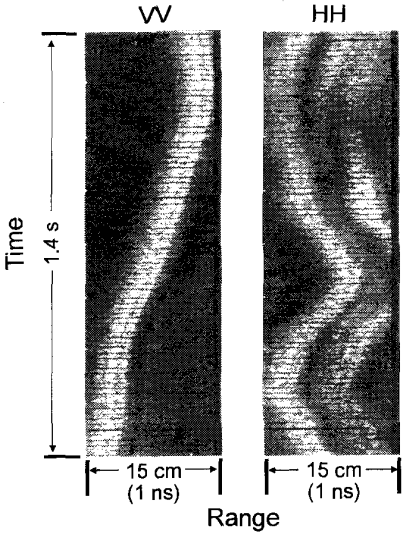


Fig. 6. Range-time plots of the VV- and HH-echo envelopes produced by the floating trihedral target. The envelope amplitude is encoded in a linear grey scale.

by simultaneous observation of the radar display and a video image of the target, the meandering of the parallel bands produced by the echo pair is mainly a result of the swell-induced drift of the target within the range swath sampled by the system. (The remainder of the range drift is an artifact of an attempt to manually adjust the fine position of the range swath, so as to keep the echo centered.) In contrast, the VV signal consists of a single echo. As seen in the bottom segment of the VV display, there is occasionally a weak echo which appears approximately 0.25 ns after the main echo, but a component with a 0.5-ns delay is not observed above the noise level of the system.

A series of 20 consecutive 1.4-s (400-waveform) averages of the power envelopes for VV and HH polarizations is displayed in Fig. 7. (To reduce the effect of the buoy drift on the averages, the leading echoes of the waveforms were aligned prior to averaging.) In the HH data, the indirect-indirect echo is readily observable and is often the same strength as the direct-direct echo. Comparison of the raw data with these 1.4-s averages shows that much of the modulation apparent in the averaged indirect-indirect echo strength is due to occasional

Authorized licensed use limited to: Perkins Coie LLP. Downloaded on June 24,2025 at 22:07:24 UTC from IEEE Xplore. Restrictions apply.

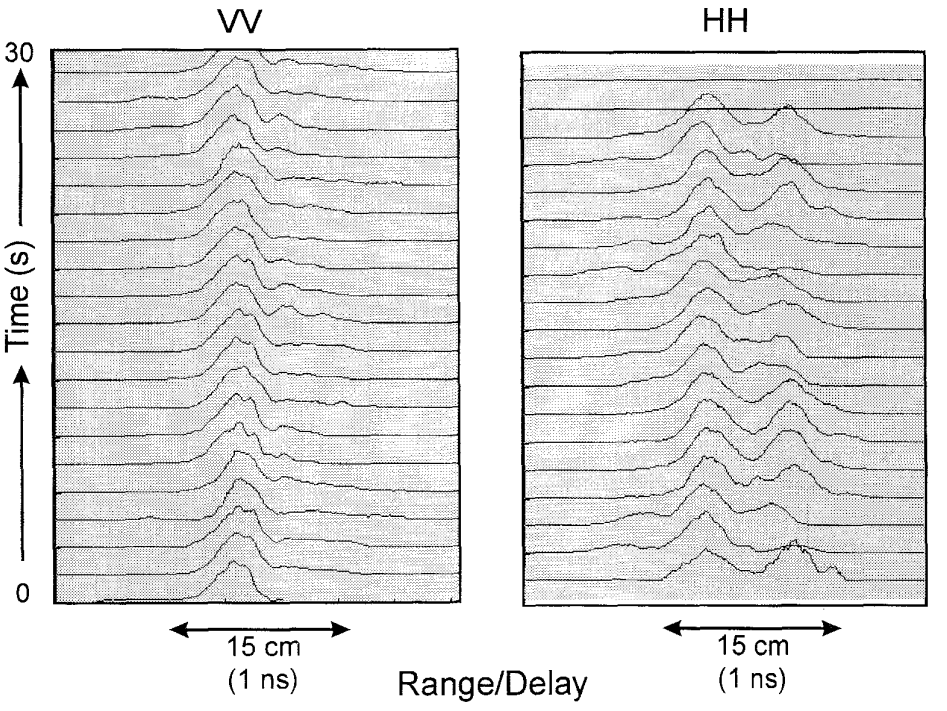


Fig. 7. 1.4–s averages of the power envelopes for VV and HH polarizations. Each average is formed from approximately 400 waveforms. The vertical scale is linear.

drifting of the target out of the range scanned by the radar. (An example of this drift can be seen approximately midway up the column of HH data in Fig. 6.) This drift is preferentially in the down-range direction which results in a reduction in the indirect-indirect echo strength after the averaging process. As shown in Fig. 7, a weak echo, located approximately 0.25 ns after the main echo, can sometimes be observed in the VV-polarized data. While this is the expected position of the direct-indirect echo from the trihedral, it is also the expected location of the echo from the small plastic float (located at the water surface, below the trihedral cluster) used for buoyancy. Given the low bistatic cross section of the trihedral and the low forward-scatter coefficient for VV polarization, it is most likely that this echo is caused by the latter.

The use of a target with a bistatic cross section higher than that for the trihedral, such as a sphere, may have allowed observation of all three multipath echoes and of the effect of Brewster-angle damping on each. However, the trihedral was chosen due to its higher (monostatic) cross section.

V. Relevance to Sea-Scatter Research

While an analysis of the role of multipath in the sea-scatter process is presented in [4], a brief synopsis of this model will be given here to provide a clearer motivation for the experiment described above. This analysis hypothesizes that for narrowband radar systems and low-grazing angles, multipath and Brewster-angle damping are major factors in the determination of the dynamic ranges of VV and HH sea scatter. Fig. 8 illustrates the theory with a simple example. Consider a scattering feature, such as a plume or bore near

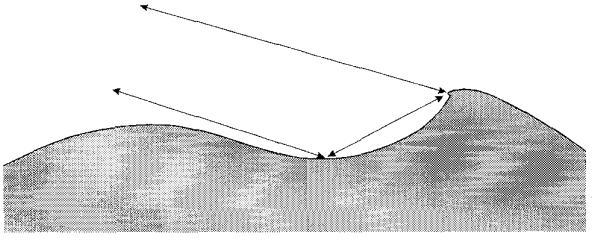


Fig. 8. Diagram illustrating the role of multipath in the generation of sea scatter. Multipath propagation may exist for strong scatterers, such as plumes or bores near the crests of breaking waves, via the underlying wave surface.

the crest of a breaking wave. Multipath propagation can occur between the scatterer and the front face of the underlying long wave. In the case of VV polarization, Brewster-angle damping limits the contributions of indirect scatter, and as a result, the measured backscatter does not exhibit significant enhancement or reduction due to multipath interference. In the case of HH polarization, however, the lack of Brewster-angle damping of the indirect paths can result in either strong backscatter enhancement or near-complete suppression, depending on the particular position of the scatterer relative to the long wave. The resulting dynamic range of the HH backscatter will consequently be significantly greater than that for VV. In addition, the model provides an explanation for "sea spikes," echoes for which the polarization ratio σ_{HH}/σ_{VV} is greater than one [3], [13]–[15].

An ultrahigh-resolution radar system provides a means by which the validity of this model can be tested. The observation of characteristic "triplicate" echoes in HH-polarized ultrawide-

Authorized licensed use limited to: Perkins Coie LLP. Downloaded on June 24,2025 at 22:07:24 UTC from IEEE Xplore. Restrictions apply.

band sea scatter data and monopulse signals (or multipulse echoes exhibiting significant damping) for VV is a necessary requirement for the establishment of the theory. While the disparity in the dynamic ranges for the two polarizations has been observed in many narrowband radar sea-clutter measurements [2], [3], [13]–[15], it is difficult to ascertain the true origin of the difference from these lower resolution measurements. Without the ability to resolve individual scatterers it is difficult to separate multipath effects from effects due to the presence of multiple scatterers within the resolution cell, or to rule out other scattering mechanisms. This experiment constitutes a first step in the verification of this theory. Given that the distance between the trihedral target and the surface is commensurate with wave heights frequently encountered on the sea, this experiment demonstrates the ability to resolve multipath components of sea-surface backscatter and verifies the effect of Brewster-angle damping on these measurements. Future experiments will concentrate on the collection of actual ultrawide-band sea scatter data.

VI. Summary

This paper discusses an experiment which uses an ultrawide-band radar system to investigate multipath propagation over the sea surface. Using the 3-cm range resolution of this x-band system, the components of a multipath signal scattered from a floating trihedral corner reflector were spatially resolved. In addition, Brewster-angle effects were observed in the indirect components of the VV-polarized backscatter in agreement with a simple model for ultrahigh-resolution multipath scattering. Both effects are believed to play important roles in the generation of sea clutter, and thus, this system provides a unique means by which the validity of sea clutter models can be investigated.

References

[1] D. K. Barton, *Radars—Volume 4: Radar Resolution and Multipath Effects.* Dedham, MA: Artech House, 1975.

[2] M. W. Long, *Radar Reflectivity of Land and Sea.* Lexington MA: Lexington Books, 1975.

[3] P. H. Y. Lee, J. D. Barter, K. L. Beach, C. L. Hindman, B. M. Lake, H. Rungaldier, J. C. Shelton, A. B. Williams, R. Yee, and H. C. Yuen, "X-band microwave backscattering from ocean waves," *J. Geophys. Res.*, vol. 100, pp. 2591–2611, Feb. 1995.

[4] D. B. Trizna, "A model for Brewster angle effects on sea surface illumination for sea scatter studies," *IEEE Trans. Geosci. Remote Sensing*, to be published.

[5] M. A. Sletten and Dennis B. Trizna, "An ultrawide-band, polarimetric radar for the study of sea scatter," *IEEE Trans. Antennas Propagat.*, vol. 42, pp. 1461–1466, Nov. 1994.

[6] M. A. Sletten and Jin Wu, "Ultrawide-band, polarimetric radar studies of breaking waves at low grazing angles," *Radio Sci.*, vol. 31, no. 1, pp. 181–192, Jan./Feb. 1996.

[7] M. A. Morgan, "Ultrawide-band impulse scattering measurements," *IEEE Trans. Antennas Propagat.*, vol. 42, pp. 840–846, June 1994.

[8] J. L. Eaves and Edward K. Reedy, *Principles of Modern Radar.* New York: Van Nostrand, 1987.

[9] J. Pete Hansen, "Experimental measurement of sea clutter using an ultrawide-band x-band radar with variable resolution," in *Ultrawide-Band Radar—Proc. SPIE 1631*, I. J. LaHaie, Ed., 1992, pp. 182–193.

[10] J. W. Crispin and K. M. Siegel, *Methods of Radar Cross-Section Analysis.* New York: Academic, 1968, p. 246.

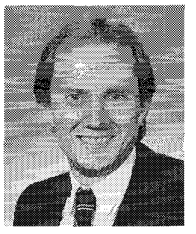
[11] C. G. Bachman, *Radar Targets.* Lexington, MA: Lexington Books, 1982, p. 81.

[12] D. E. Kerr, Ed., *Propagation of Short Radio Waves.* Lexington, MA: Boston Tech. Publ., 1964, pp. 402–403.

[13] A. I. Kalmykov and V. V. Pustovoytenko, "On polarization features of radio signals scattered from the sea surface at small grazing angles," *J. Geophys. Research*, vol. 81, pp. 1960–1964, Apr. 1976.

[14] B. L. Lewis and I. D. Olin, "Experimental study and theoretical model of high-resolution backscatter from the sea," *Radio Sci.*, vol. 15, pp. 815–828, July 1980.

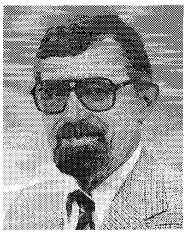
[15] D. J. McLaughlin, N. Allan, and E. M. Twarog, "High resolution polarimetric radar scattering measurements of low grazing angle sea clutter," *IEEE J. Oceanic Eng.*, vol. 20, pp. 166–178, July 1995.



Mark A. Sletten (S'87–M'91) received the B.S., M.S., and Ph.D. degrees in electrical engineering from the University of Wisconsin, Madison, in 1984, 1987, and 1991, respectively.

From 1985–1987, he was a Research Assistant and ECE Department Fellow at the Wisconsin Center for Applied Microelectronics, University of Wisconsin, Madison, involved in the development of silicon-based optical detectors. He held internships at Hewlett-Packard's integrated circuit research facility in Corvallis, OR, during his undergraduate and graduate studies. As a Doctoral Student under the Rockwell International Graduate Fellowship Program, his research included theoretical and experimental investigations of polarization-altering guided wave-optical devices. Since joining the Naval Research Laboratory, Washington, DC, in 1991, his research has included the development of ultrawide-band polarimetric radar systems and their application to sea scatter, as well as the development of laser-based instruments for the measurement of water-surface morphology.

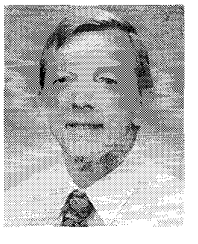
Dr. Sletten is a member of Eta Kappa Nu, Tau Beta Pi, and the IEEE Antennas and Propagation Society.



Dennis B. Trizna (M'82) received the B.S. degree in physics from Illinois Benedictine College, Lisle, IL, in 1963, and the Ph.D. degree in physics from Iowa State University, Ames, IA, in 1970.

In 1970, he joined the Naval Research Laboratory (NRL) Radar Division, Washington, DC. He began his career at the NRL in the area of over-the-horizon (OTH) HF radar. He copublished the first map of a weather system at sea, using OTH radar propagation, and later published the first map of surface currents of the gulf stream and eddies, using OTH radar. He subsequently developed a model for second-order Doppler characteristics of HF sea echo spectra. In addition to other applied HF radar studies of interest to the Navy, he has worked in the areas of microwave propagation and radar sea-scatter mechanisms, and has developed the use of marine radars to measure sea-surface parameters. His most recent areas of interest have been both field and laboratory studies of radar sea scatter from breaking waves, using polarimetric and ultrawide-band radars and laser-scanning slope gauges to quantify their scattering sources.

Dr. Trizna has served, for the past three years, and continues to serve (part time) as Program Officer for the Remote Sensing Program at the Office of Naval Research, Washington, DC. He is a member of the American Geophysical Society and the American Physical Society.



James P. Hansen (S'62–M'65) received the B.S. degree in electronics from George Washington School of Engineering, Washington, DC, in 1964.

He is an Electronics Engineer, specializing in experimental research and has worked in the Radar Division of the Naval Research Laboratory, Washington, DC, since 1964. He has published papers in the areas of rain clutter, adaptive cancellation, coherent signal processing, laser radar, and wideband radar technology. He holds 13 patents.

Authorized licensed use limited to: Perkins Coie LLP. Downloaded on June 24,2025 at 22:07:24 UTC from IEEE Xplore. Restrictions apply.